

Monohydroxy-Hydrazone-Functionalized Thermally Crosslinked Polymers for Nonlinear Optics

Rajendra K. Singh,¹ James O. Stoffer,¹ Tony D. Flaim,² David B. Hall,³ John M. Torkelson³

¹Department of Chemistry, University of Missouri–Rolla, Rolla, Missouri 65401

²Brewer Science, Inc., P.O. Box GG, Rolla, Missouri 65402

³Department of Chemical Engineering, Northwestern University, Evanston, Illinois 60208

Received 3 December 2002; accepted 27 June 2003

ABSTRACT: The synthesis and properties of six hydrazone-functionalized crosslinked polymers possessing stable nonlinear optics (NLO) properties are presented. First, a series of six hydroxy-functionalized, NLO-active hydrazone chromophores were synthesized. These chromophores were then grafted via its hydroxy functionality on an epoxy polymer to obtain the six NLO-active soluble prepolymers. The grafting reaction yielded multiple secondary hydroxyl sites, which were used for further crosslinking by formulation of the prepolymer with a blocked polyisocyanate crosslinker.

This formulation was spin-coated on glass slides to form 2–2.5 μ thick defect-free transparent films. The films were corona-poled above their glass-transition temperatures to align the chromophores in a noncentrosymmetric fashion and were simultaneously cured. The thermal characteristics of the second-order nonlinearity of the six polymers were compared to illustrate the key structure–property relationships underlying the performance of the films in terms of NLO activity and thermal stability. © 2004 Wiley Periodicals, Inc. *J Appl Polym Sci* 92: 770–781, 2004

INTRODUCTION

Electronic materials, which have been at the heart of the telecommunication industry, are fast approaching their limitations, and soon, photonics will be the key in revolutionizing the telecommunication industry. The area of nonlinear optics (NLO) is a rapidly progressing field of science and technology that has the potential to offer unparalleled switching speed and bandwidth for optical signal processing.¹ One of the major hurdles to the realization of second-order NLO polymer devices has been overcoming the loss of noncentrosymmetric order within the molecular structures at elevated manufacturing and operating temperatures. Most of the current systems invariably exhibit relaxation of the dipole alignment at temperatures as low as room temperature. Major efforts are underway to synthesize amorphous polymers possessing good second-order optical nonlinearity (χ^2), with particular interest centered around polymers that incorporate NLO-active chromophores into the polymeric structure as opposed to the preparation of simple doped (or guest-host) polymer systems.² Because χ^2 is directly proportional to the concentration of the NLO-active chromophores, the attachment of groups directly to the polymer allows a higher

chromophore concentration and subsequent higher χ^2 values.³

The final glass-transition temperature (T_g) seems to be the critical parameter in the definition of the long-term stability of the poling-induced optical nonlinearity. Relaxation phenomena, which govern the lifetime of a poled polymer device, can be controlled either by the enhancement of the T_g of the polymer system or the improvement of the extent of polymer-chain interactions. However, it is not feasible to use polymers with very-high- T_g 's, because chromophore decomposition often occurs before an effective poling temperature can be attained. A more optimal system is a material with a moderately high T_g , which can be easily processed into good optical quality film and then poled at practical temperatures and, can be subsequently, hardened via thermal crosslinking to achieve long-term stability. A very important condition required for such a system would be that most of the crosslinking occur either during or after the poling process and not prior to that point. The necessity of this requirement is simply to ensure that the poled orientation requires dipole mobility, but if crosslinking precedes chromophore poling, the poling would not be completed due to the partial chain immobilization caused by crosslinking. Furthermore, the crosslinking process must not degrade optical quality (transparency), which could result in mechanical stress or a significant shrinkage of the system.

Temporal stability, which is the stability of the overall poled orientation of a NLO-active polymer, can also be enhanced by the induction of a certain degree

Correspondence to: J. O. Stoffer (jstoffer@umr.edu).

TABLE 1
Structures of Hydrazones I–VI

Hydrazone	Structure	Yield (%)	mp (°C) ^a
I		76	273
II		70	198.5
III		78	231.9
IV		89	284.2
V		83	266.8
VI		72	230.2

^a Measured by DSC at a heating rate of 10°C/min; the maximum melting peak on DSC is reported as the mp.

of crosslinking. In crosslinked polymers, the NLO-active chromophores are locked in a rigid crosslinked network, which reduces its overall mobility and makes it difficult for them to relax into a random orientation. Such an approach was first reported by Eich et al.⁴ and this novel concept was then used by a number of other research groups.^{5–9} Jungbauer et al.¹⁰ reported a chemically crosslinked epoxy-chemistry-based NLO-active polymer matrix yielding significant temporal stability.

We further explored this concept by synthesizing a series of hydrazone-functionalized NLO polymers. The resulting polymers were then formulated with a blocked polyisocyanate crosslinking agent to form a thermally curable coating. High dipole mobility was maintained during the poling process in these systems through control of the precure T_g and poling temperature so that both were below the temperature required for final curing. The T_g values for the six NLO polymers fell in the range 127–147°C. However, the crosslinking reaction occurred only above 150°C because the deblocking temperature of the blocked polyisocyanate was 149°C; thus, poling concurrent with crosslinking was achieved. Our approach focused on

the use of hydrazone chromophores that could easily be synthesized and subsequently incorporated into a commercial epoxy polymer system. Our goal was to provide a systematic variation of the chromophore structure and to study its effect on the optical nonlinearity and thermal stability of the final crosslinked system.

Aromatic hydrazones are known to exhibit good NLO activity. The NLO activity of hydrazone derivatives have been investigated in detail as crystals and as Langmuir–Blodgett films,^{11–14} as characterized by the Kurtz and Perry¹⁵ powder test. A typical hydrazone functionality consists of a secondary amino nitrogen atom bearing three single σ bonds, with a lone pair of electrons, conjugated with the π electron system of the adjacent $sp^2N=sp^2C$ azomethine functionality. This arrangement results in a configuration that yields a planar trigonal amino nitrogen, which makes the hydrazone backbone into a asymmetric transmitter, with charge transfer occurring between the electron-donating and electron-withdrawing groups by cross-conjugation through the central planar amino nitrogen.¹⁶ Serbutoviez et al.¹⁴ synthesized a series of 39 hydrazone derivatives and found that a very high number of

them exhibited positive second-harmonic signals in the powder test. Bolognesi et al.¹⁷ reported preliminary results that they obtained in an investigation on several organic compounds, among which they found that *p*-nitrophenylhydrazine (*p*-NPH) appeared to be as good a second-harmonic generator (SHG) as 2-methyl-4-nitroaniline. Further work by Pandarese et al.¹⁸ showed an increase in the intensity of SHG in *p*-NPH between room temperature and 77 K. Following this, Bertinelli and Taliani¹⁹ published some optical and spectroscopic data of *p*-NPH with the intention of providing new experimental evidence that could lead to better knowledge of its NLO properties. Owen and White²⁰ were the first to report a relative SHG efficiency of hydrazone compounds synthesized by the coupling of *p*-NPH with carbonyl compounds. Kminek and Nespurek²¹ focused achieving the improved thermal stability of NLO-active hydrazone chromophores by incorporating them into certain polymer systems. Their work involved synthesis of 2,4-dinitrophenylhydrazone of partially formylated polystyrene, which photocrosslinks and undergoes thermal crosslinking. In addition, they prepared the benzaldehyde-4-nitrophenylhydrazone derivative of partially formulated polystyrene as a potential NLO material. During ultraviolet radiation and/or heating near T_g , the authors expected the polymer to crosslink via the azomethine group ($-\text{CH}=\text{N}-$) of the hydrazone chromophore and to form partially or fully saturated nitrogen-containing heterocycles. The crosslinking resulted in bleaching, which was an indication that the chromophore suffered considerable damage during the crosslinking process. Because it is important to keep the chromophore concentration very high for SHG applications of poled films, the authors concluded that it was important to find poling conditions that would cause none or only minor damage to the NLO-active chromophores and yet would permit crosslinking to proceed to an extent sufficient for stabilization of the poled system.

EXPERIMENTAL

Materials

The starting materials used in the synthesis of the six hydrazones, as shown in Table 1, namely, the six carbonyl compounds and the two phenylhydrazines, were commercially available compounds (Aldrich Chemical Co.) and were used as received. All of the solvents and other chemicals were also used without further purification. The epoxy resin, EPON DPS-164, was obtained from Shell Chemical Co., and the blocked polyisocyanate crosslinker Desmodur BL-3175A was from Miles, Inc.; both were used as supplied.

Fourier transform infrared (FTIR) spectroscopy was performed with a Nicolet Magna-IR system 750 spec-

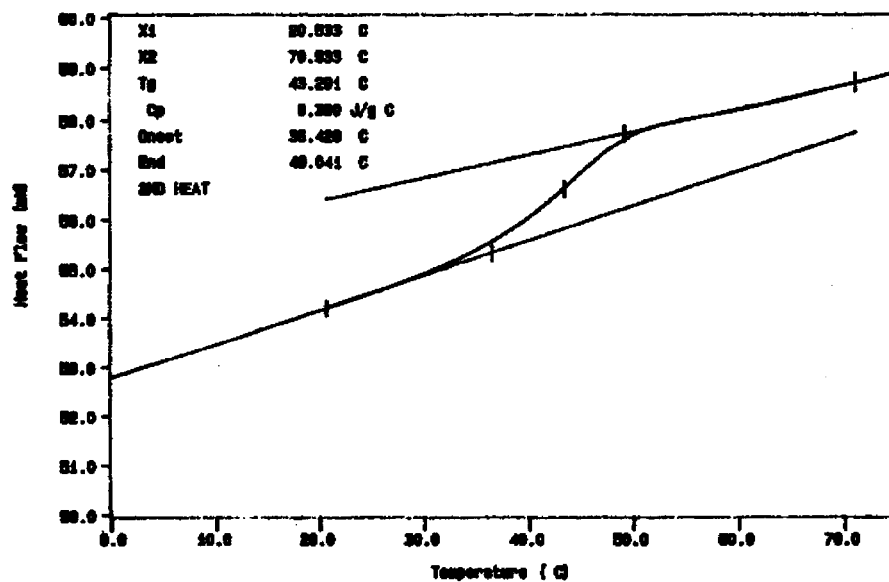
trometer. Midinfrared (MIR) data was collected via potassium bromide (KBr) pellets with a KBr beam splitter, an IR source, and a DTGS KBr detector. Near infrared (NIR) data was obtained via calcium fluoride (CaF_2) pellets with a CaF_2 beam splitter, a white light source, and a PbSe detector. Analysis was performed in transmission mode, with 32 scans collected at a resolution of 4 cm^{-1} . Data manipulation included automatic baseline correction and magnification of the relevant spectral region. Melting point (mp) determination of all of the hydrazones was done on a TA Instruments 2010 differential scanning calorimeter under a nitrogen atmosphere at a heating rate of $10^\circ\text{C}/\text{min}$. The differential scanning calorimeter was calibrated with an Indium standard. T_g measurements were also performed on a differential scanning calorimeter at a heating rate of $20^\circ\text{C}/\text{min}$. Because the T_g values of all six NLO-active epoxy polymers were below 200°C , all of the samples were heated initially to 200°C , then quickly quenched with liquid nitrogen, and reheated to 200°C to observe T_g of the polymer. The T_g was taken at the inflection point of the ΔT versus temperature curve.

Thin-layer chromatography (TLC)

Incorporation of hydrazones into EPON 164 was monitored by a simple TLC technique. For TLC, the specific incorporated hydrazone and the hydrazone incorporated NLO-active reaction mixture were spotted and developed in a 2 : 1 ethyl acetate:hexane solvent mixture. The almost negligible presence of the starting hydrazone in the NLO-active resin spot confirmed the completion of the reaction. A comparison of the TLC spotting for the deionized-water-washed and ethanol (EtOH)-washed NLO-active resin was used to evaluate the presence of unreacted hydrazone. This evaluation confirmed the necessity of stirring the precipitated polymer solids in EtOH to remove the final traces of unreacted hydrazone that also precipitated during the reaction workup.

Differential scanning calorimetry (DSC)

DSC output, as shown in Figure 1, confirmed the specified T_g of commercial EPON 164 as listed by the vendor. The T_g values of the six NLO-active systems (NLOs I–VI) are shown in Table II, and the T_g data output for NLO I is shown in Figure 2. The decreasing order of T_g values for the series was as follows: NLO 1 > NLO IV > NLO VI > NLO III > NLO V > NLO II. This order indicated that the epoxy resins incorporated with hydrazones made from the benzaldehyde carbonyl compounds (NLOs I and IV) had the highest T_g , followed by the benzophenone carbonyl hydrazones (NLOs III and VI); the lowest T_g was for the acetophenone carbonyl hydrazones (NLOs II and V).

Figure 1 T_g of EPON 164.

To confirm the absence of any T_g for the crosslinked epoxy system, aliquots of each formulation containing the NLO polymer with blocked polyisocyanate were pipetted into a aluminum weighing cup and were then placed in a oven maintained at 150°C for 30 min. Because the deblocking temperature of the crosslinker Desmodur BL-3175A was 149°C, the formulation aliquots were heated in a 150°C oven. After 30 min of heating, the specimens became rigid crosslinked composite solids. Tiny flakes of these solids were chipped off to run DSC scans to determine the presence of T_g 's. The chipped flakes were heated 300°C in the DSC, but none of the six crosslinked systems exhibited any thermal transition, thus confirming that all of the formulations had undergone a crosslinking reaction.

NIR measurements of NLO-active epoxy resins

FTIR spectroscopy can be useful in monitoring the cure reactions of epoxy resins. The functional group of interest in the epoxy resin cure reaction generally has well-isolated absorption bands in the NIR region of

the spectrum, ranging from 7000 to 4000 cm^{-1} . This region encompasses bands resulting from the harmonic overtones of fundamental and combination bands. In the late 1950s, Goddu and Delker²² identified two characteristic bands in the NIR region (6061 and 4546 cm^{-1}) for the terminal epoxide group. In 1963, Dannenberg²³ investigated epoxy-amine cure reactions via NIR spectroscopy to study the reaction of diglycidylether of bisphenol A (DGEBA) with *m*-phenylenediamine. Similarly, Schiering and Kanton²⁴ utilized NIR spectroscopy to study the reaction of DGEBA with *m*-phenylenediamine. The authors used peaks in the MIR region (914 cm^{-1}) as well as the peak in the NIR region (4530 cm^{-1}) to quantify the terminal epoxide bands. In 1995, Mijovic and Andjelic^{25,26} made a direct comparison of NIR and MIR spectra and concluded that the standard MIR epoxy absorption of 915 cm^{-1} was not an exclusive measure of free epoxy groups and was affected by other absorption mechanisms, including hydrogen bonding and overlapping group absorption. The authors also proved conclusively that NIR spectroscopy was an attractive method for qualitative and quantitative evaluation for monitoring the progress of an epoxy ring-opening reaction. They focused their attention on the NIR region containing the combination band of epoxy stretching and bending vibration at 4530 cm^{-1} for kinetic studies because the absorption intensity of that peak decreases systematically with progress in the reaction.

In this investigation, NIR spectroscopy was utilized to qualitatively confirm the completion of the hydroxy-initiated epoxide ring-opening reaction through the disappearance of the 4525–4530 cm^{-1} peak. Figure

TABLE II
 T_g of EPON 164 and NLOs I-VI

System	T_g (°C) ^a
EPON 164	43.3
NLO I	147.6
NLO II	127.0
NLO III	137.2
NLO IV	143.0
NLO V	128.2
NLO VI	137.3

^a Heating rate = 20°C/min.

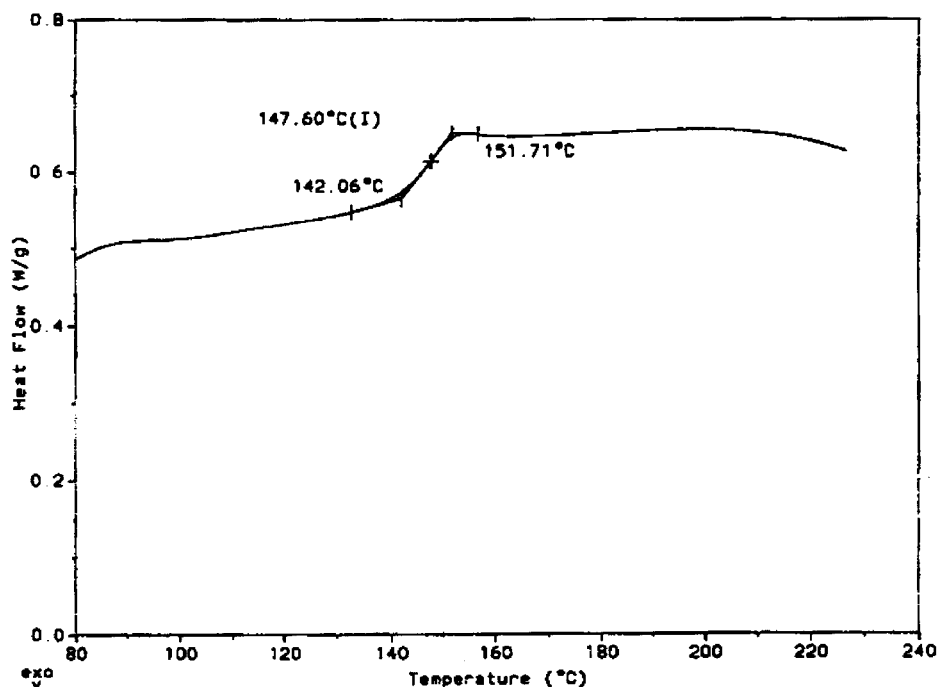


Figure 2 T_g of NLO I.

3 shows the NIR spectrum of the commercial EPON 164 resin with the relevant 4526 cm^{-1} epoxy ring peak marked. Figure 4 shows a combination of EPON 164 and NLO 1 spectra that revealed the near absence of the characteristic epoxy ring peak at 4526 cm^{-1} .

Formulation and spin coating

The reaction of hydrazones I–VI with the epoxide rings on EPON 164 yielded a soluble prepolymer with multiple secondary hydroxyl groups. These hydroxyl

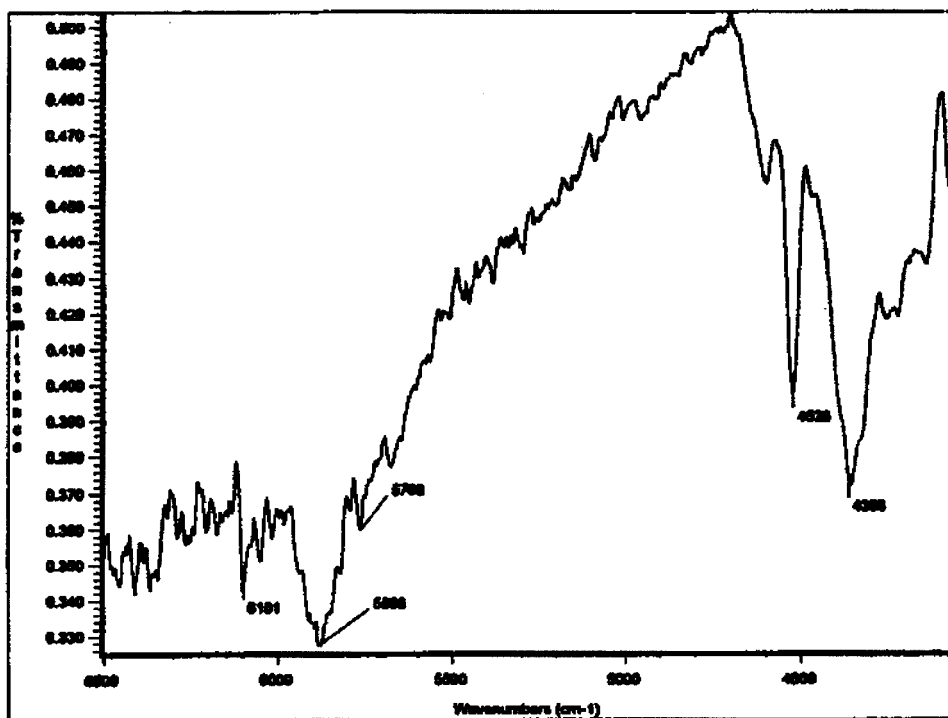


Figure 3 NIR spectrum of EPON 164.

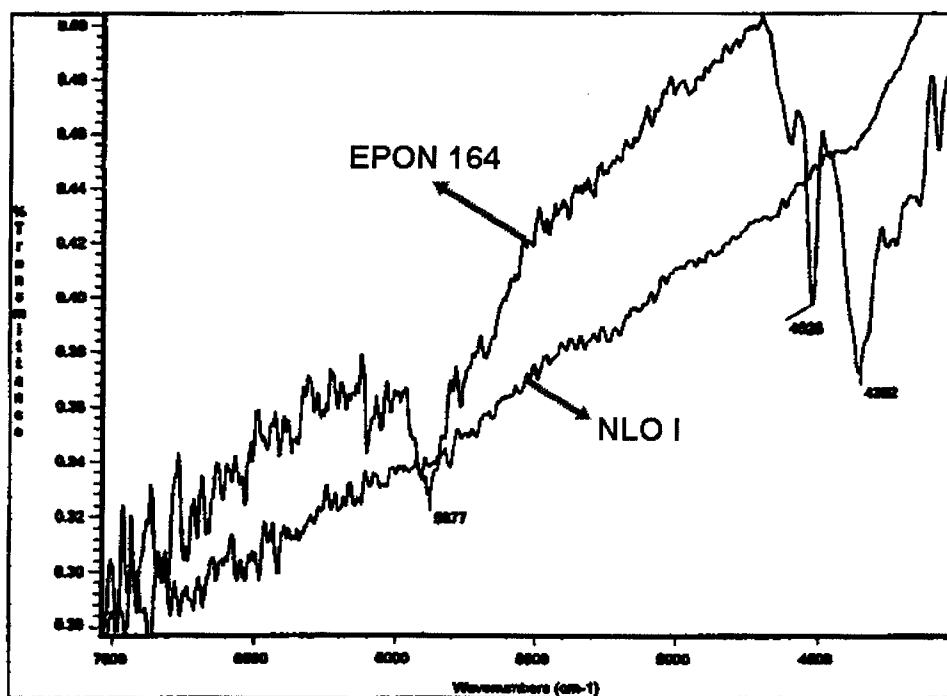


Figure 4 NIR of EPON 164 and NLO I.

groups were subsequently used as potential crosslinking sites by formulation with a commercial polyisocyanate crosslinker called Desmodur BL-3175A from Miles, Inc. BL-3175A is a blocked aliphatic polyisocyanate based on hexamethylene diisocyanate with a deblocking temperature of 149°C. It is obtained as a 75 wt % solid solution with an average equivalent weight of 370. The hydrazone functionalized prepolymers, NLO I–VI, were formulated at 1 : 1 stoichiometry with BL-3175A on the basis of their respective equivalent weights. All of the formulations were stirred overnight and then filtered through a 0.2- μm endpoint filter Whatman to remove particles. The filtered solutions were spin-coated on clean glass slides via the conventional spin-coating technique used in microfabrication. The coated solutions were spun at appropriate speeds to obtain 2–2.5 μm thick optically clear, uniform, defect-free films. The films were then baked on a hot plate maintained at 100°C for 60 to get rid of solvents and were then dried overnight in a vacuum oven at 100°C to ensure the complete removal of all residual solvent.

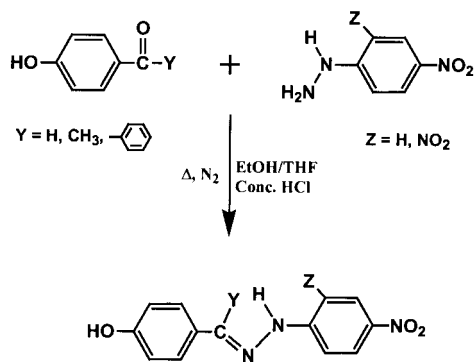
Corona poling

The spun films were staged to a final temperature above their T_g and then corona-poled under a high field^{27–29} to orient the hydrazone chromophores non-centrosymmetrically. The coated slides were placed on the poling apparatus at room temperature. The poling current was increased to 2 μA , and the temperature

was ramped to 100°C. This set temperature and current were kept constant for 10 min, after which the temperature was ramped to the minimum deblocking temperature of the crosslinker (150°C) with the current held constant. Films were cured for 30 min at this temperature and were then cooled slowly to room temperature, after which the current was removed. Ramping studies were performed to evaluate the stability of the signal as a function of temperature. The film side of each slide was oriented away from the laser (Nd : YAG), and the fundamental light intensity was reduced through use of filters before the ramp studies were started. Initially, the background for both the SHG signal and the reference was adjusted to approximately 5 mV. Subsequently, the signal reference was adjusted to approximately 190 mV and the SHG signal to approximately 290 mV. Ramping studies were initiated at room temperature and concluded when the SHG signal reached background level.

Synthesis of hydrazones I–VI

The complete setup included a 250-mL three-necked round-bottomed flask (RBF) containing an oval-shaped magnetic stir bar and fitted with a water condenser, nitrogen inlet, and thermometer. The RBF was heated with a heating mantle, which was connected to a Variac to control temperature. This setup was used in the synthesis of each of the six hydrazones and also for incorporation of the hydrazones into the commercial epoxy resin to obtain the corresponding six NLO-



Scheme 1 General hydrazone synthesis reaction.

active hydrazone-functionalized epoxy polymers. A general reaction scheme illustrating the coupling of a hydrazine with a carbonyl compound to form a hydrazone is shown in Scheme 1.

4-Hydroxybenzaldehyde-4-nitrophenylhydrazone (hydrazone I)

Exactly 11.25 g (0.073 mol) of 4-nitrophenylhydrazine (4-NPH) was weighed in a RBF followed by the addition of 80 mL of a 3 : 1 EtOH : tetrahydrofuran (THF) solvent mixture. This mixture was stirred and heated to reflux, but because 4-NPH was not totally soluble, drops of concentrated hydrochloric acid (HCl) were slowly added to the refluxing mixture. After the addition of 1.3 g of HCl, complete dissolution occurred; then, 9.16 g (0.075 mol) of 4-hydroxybenzaldehyde was slowly added into the stirring solution. Within 5 min, after the complete addition of the carbonyl compound, precipitation of hydrazone I occurred, causing a reduction in the stirring rate. To ensure smooth stirring, an additional 20 mL of the EtOH : THF solvent mixture was added, and we continued to reflux the mixture. After refluxing for 4 h, the hot solution was vacuum-filtered to collect the maroon solid, which was dried overnight *in vacuo* at 75°C. The final yield obtained was 14.3 g (76%), and the maximum mp peak of the final product, as determined by DSC, was 273°C. TLC spotting of both the reactants and the final product confirmed the purity of hydrazone I.

4'-Hydroxyacetophenone-4-nitrophenylhydrazone (hydrazone II)

Exactly 11.25 g (0.073 mol) of 4-NPH was weighed in a RBF followed by the addition of 40 mL of EtOH. This mixture was stirred and heated to reflux, but because 4-NPH was not totally soluble, drops of concentrated HCl were slowly added to the refluxing mixture. After the addition of 2.0 g of HCl, complete dissolution occurred; then, 10.21 g (0.075 mol) of 4'-hydroxyacetophenone was slowly added into the stirring solution

and finally rinsed with 15 mL of EtOH. After refluxing for 8–10 h, the heat was turned off, and the solution was allowed to cool to room temperature. On cooling, slow precipitation occurred, and this final product was vacuum-filtered to obtain a dark maroon gaze-textured solid, which was dried overnight *in vacuo* at 75°C. The final yield was 13.9 g (70%), and the maximum DSC mp peak was 198.5°C. TLC spotting of both the reactants and the final product confirmed the purity of hydrazone II. The synthesis of hydrazone II was performed in EtOH only because three runs, with varying amounts the EtOH : THF solvent mixture resulted in low yields, and the highest yield achieved with this solvent mixture was only 53%.

4-Hydroxybenzophenone-4-nitrophenylhydrazone (hydrazone III)

Exactly 11.25 g (0.073 mol) of 4-NPH was weighed in a RBF followed by the addition of 75 mL of EtOH. This mixture was stirred and heated to reflux, but because 4-NPH was not totally soluble, drops of concentrated HCl were slowly added to the refluxing mixture. After the addition of 2.0 g of HCl, complete dissolution occurred; then, 14.85 g (0.075 mol) of 4-hydroxybenzophenone was slowly added into the stirring solution, and finally, the solution was rinsed with 25 mL of EtOH. The reaction solution was refluxed overnight and then cooled, after which precipitation of the product occurred. The final product was vacuum-filtered to obtain an orange solid, which was dried overnight *in vacuo* at 75°C. The final yield was 19.0 g (78%), and the maximum DSC mp peak was 231.9°C. TLC spotting of both the reactants and the final product confirmed the purity of hydrazone III.

4-Hydroxyaldehyde-2,4-dinitrophenylhydrazone (hydrazone IV)

Exactly 23.18 g (0.117 mol) of 2,4-dinitrophenylhydrazine (2,4-DNPH) was weighed in a RBF followed by the addition of 100 mL of THF. Commercial 2,4-DNPH contained at least 30% moisture, which was taken into account for stoichiometry calculations. This mixture was stirred and heated to reflux, but because 2,4-DNPH was not totally soluble, drops of concentrated HCl were slowly added to the refluxing mixture. After the addition of 3.6 g of HCl, complete dissolution occurred; then, 10.00 g (0.082 mol) of 4-hydroxybenzaldehyde was slowly added into the stirring solution, and the solution was finally rinsed with 45 mL of THF. Within 10 min, after the complete addition of the carbonyl compound, precipitation took place. The reaction solution continued to be refluxed for 4 h, and it was then vacuum-filtered to obtain a brick red solid, which was dried overnight *in vacuo* at 75°C. The final yield was 22.0 g (89%), and the maximum DSC mp

peak was 284.2°C. TLC spotting of both the reactants and the final product confirmed the purity of hydrazone IV.

4'-Hydroxyacetophenone-2,4-dinitrophenylhydrazone (hydrazone V)

Exactly 12.5 g (0.063 mol) of 2,4-DNPH was weighed in a RBF followed by the addition of 100 mL of a 1 : 1.5 EtOH : THF solvent mixture. This solution was stirred and heated to reflux, but because 2,4-DNPH was not totally soluble, drops of concentrated HCl were slowly added to the refluxing mixture. After the addition of 6.0 g of HCl, complete dissolution occurred, then, 5.60 g (0.041 mol) of 4'-hydroxyacetophenone was slowly added into the stirring solution, and the solution was finally rinsed with 25 mL of the solvent mixture. After this solution was refluxed for 8–10 h, the heat was turned off, and it was allowed to cool slowly to room temperature. On cooling, slow precipitation occurred, and this final product was vacuum-filtered to obtain shiny maroonish solid, which was dried overnight *in vacuo* at 75°C. The final yield was 10.82 g (83%), and the maximum DSC mp was 266.8°C. TLC spotting of both the reactants and the final product confirmed the purity of hydrazone V.

4-Hydroxybenzophenone-2,4-dinitrophenylhydrazone (hydrazone VI)

Exactly 12.5 g (0.063 mol) of 2,4-DNPH was weighed in a RBF followed by the addition of 100 mL of a 1 : 1.5 EtOH : THF solvent mixture. This solution was stirred and heated to reflux, but because 2,4-DNPH was not totally soluble, drops of concentrated HCl were slowly added to the refluxing mixture. After the addition of 5.72 g of HCl, complete dissolution occurred; then, 8.13 g (0.041 mol) of 4-hydroxybenzophenone was slowly added into the stirring solution, and the solution was finally rinsed with 25 mL of solvent mixture. The reaction solution was refluxed overnight and then cooled slowly to room temperature. On cooling, slow precipitation occurred, and this final product was vacuum-filtered to obtain a shiny reddish orange solid, which was dried overnight *in vacuo* at 75°C. The final yield was 11.2 g (72%), and the maximum DSC mp was 230.2°C. TLC spotting of both the reactants and the final product confirmed the purity of hydrazone VI.

Synthesis of hydrazone-functionalized epoxy prepolymers

The reaction setup was the same as that used for the synthesis of the six hydrazones. The basic experimental procedure, as described next for NLO I, was followed for the synthesis of all six hydrazone-function-

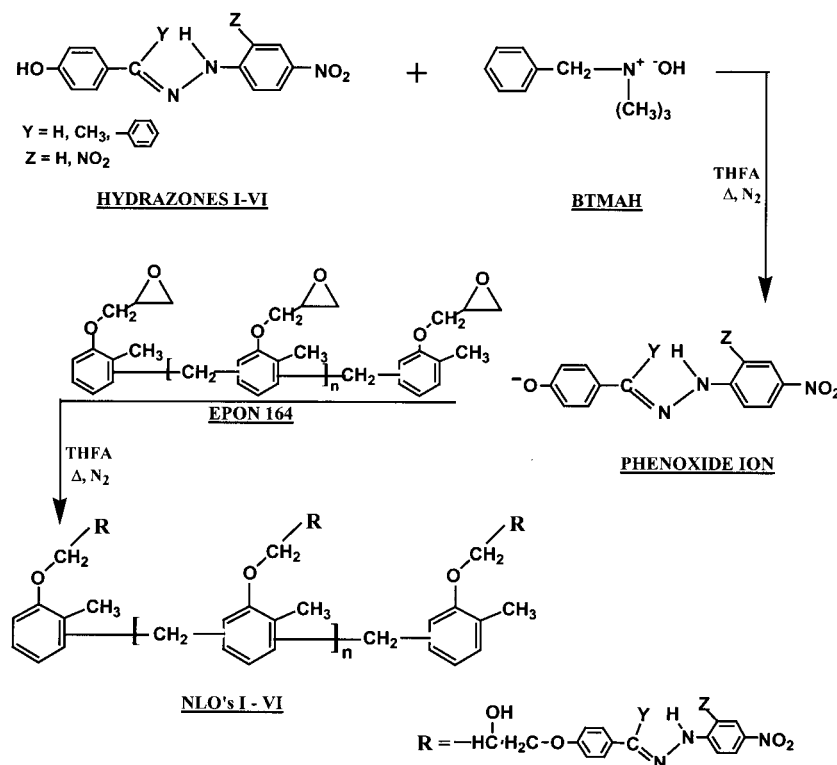
alized epoxy polymers. A general reaction scheme illustrating the incorporation of a hydrazone into an epoxide (EPON 164) to form the NLO-active prepolymer is shown in Scheme 2. Table III lists the exact amount of reactants and solvents used, including the color of the final polymer solids.

NLO I

Exactly 20.0 g of hydrazone I (0.078 mol) was weighed into a smooth stirring 50-mL of tetrahydrofurfuryl alcohol (THFA), and the walls of the RBF were rinsed down with an additional 25 mL of THFA. This mixture was heated to 155°C, where complete dissolution occurred, and afterwards 1.63 g (0.004 mol) of the base catalyst benzyltrimethylammonium hydroxide (BTMAH) was dripped into the mixture BTMAH is a 40% solution in methanol, and this had to be taken into account during stoichiometry calculations. When the reaction solution was at 165°C, 19.0 g of EPON 164 was slowly added over a period of 45 min to the stirring reaction mixture. This mixture was heated overnight at 165–168°C. For workup of the solution, the temperature was first reduced to 125°C before the addition of 0.74 g (0.004 mol) of *p*-toluenesulfonic acid monohydrate (*p*-TSA · H₂O). We continued to stir this mixture at 125°C for an additional 2 h, after which we worked it up by pouring the solution into a spark-free blender containing 250 mL of deionized water. This caused precipitation of orangish brown polymer solids, which were collected by vacuum filtration and immediately stirred in hot deionized water to dissolve any salt formation from the neutralization of the base catalyst with *p*-TSA · H₂O. The polymer was collected via vacuum filtration and dried overnight *in vacuo* at 75°C. The dried polymer solid was then stirred for 4–6 h in EtOH at room temperature to get rid of any unreacted hydrazone I. The absence of hydrazone I was confirmed by the TLC spotting of THFA solutions of hydrazone I and NLO I.

RESULTS AND DISCUSSION

There are many discrepancies in the literature concerning the physical properties of 2,4-dinitrophenylhydrazone. Geometrical (*syn*–*anti*) isomerism in arylhydrazones is well known^{30,31} and is mostly responsible for the large number of discrepancies concerning the mp values of dinitrophenylhydrazones. Careful investigation has indicated that the choice of hydrochloric acid or sulfuric acid, as the acid catalyst, is the primary cause of multiple mp values for the same dinitrophenylhydrazone. Acetaldehyde gives a dinitrophenylhydrazone that seems to exist in two forms, one with a mp of 147°C and the other with a mp of 164°C.³² In at least five comparable runs, the use of hydrochloric acid always gave a crude product with a



Scheme 2 General synthesis reaction for NLOs I-VI.

mp of 157°C or higher, but the use of sulfuric acid always resulted in the low-mp product. Bryant³³ assumed that the two were polymorphs, whereas Campbell³⁴ insisted that this was a case of insufficient purification. Bredereck³⁵ suggested the occurrence of geometrical isomerism and demonstrated the same in the furan series. The change of one form into the other was catalyzed by acidic reagents, and chances of this occurring were higher in the sulfuric acid procedure, in which the acid was more difficult to remove during purification.

The separation of dinitrophenylhydrazones from unused reagent is often difficult. In view of this, Allen and Richmond³² suggested the use of a slight excess of the carbonyl compound. According to the authors, most of the discrepancies in mp values in literature is possibly due to the contamination of the derivative

with the reagent. One of the six monohydroxy hydrazones synthesized in this investigation was 4-hydroxy-benzaldehyde-2,4-dinitrophenylhydrazone (hydrazone IV), which exhibited a maximum mp peak (DSC) of 284.2°C (Fig. 5). The synthesis of the same hydrazone was listed in the literature by two research groups, who reported different mp values of 270–271°C³⁶ and 284–284.5°C.³⁷ Johnson,³⁶ who reported the lower mp, synthesized the hydrazone with a phosphoric acid–EtOH solution of 2,4-DNPH, whereas Shine,³⁷ who reported the higher mp, used a hydrochloric acid–diglyme solution of 2,4-DNPH. In this work, the synthesis of hydrazone IV was carried out in an EtOH–THF solution of 2,4-DNPH acidified with hydrochloric acid, and thus, its mp closely matched the one reported by Shine. On the basis of all the literature findings and conclusions, the synthesis of all

TABLE III
Synthesis of Hydrazone-Functionalized Epoxy Prepolymers

	NLO II	NLO III	NLO IV	NLO V	NLO VI
Hydrazone (g)	21	23	20	20	20
THFA (mL)	70	70	85	95	70
BTMAH (g)	1.62	1.44	1.38	1.32	1.11
EPON 164 (g)	8.92	16.87	16.17	15.46	12.92
<i>p</i> -TSA · H ₂ O (g)	0.74	0.66	0.63	0.6	0.5
Final product color	Brown	Fibrous light mustard	Granular candy brown	Maroon	Fibrous candy brown

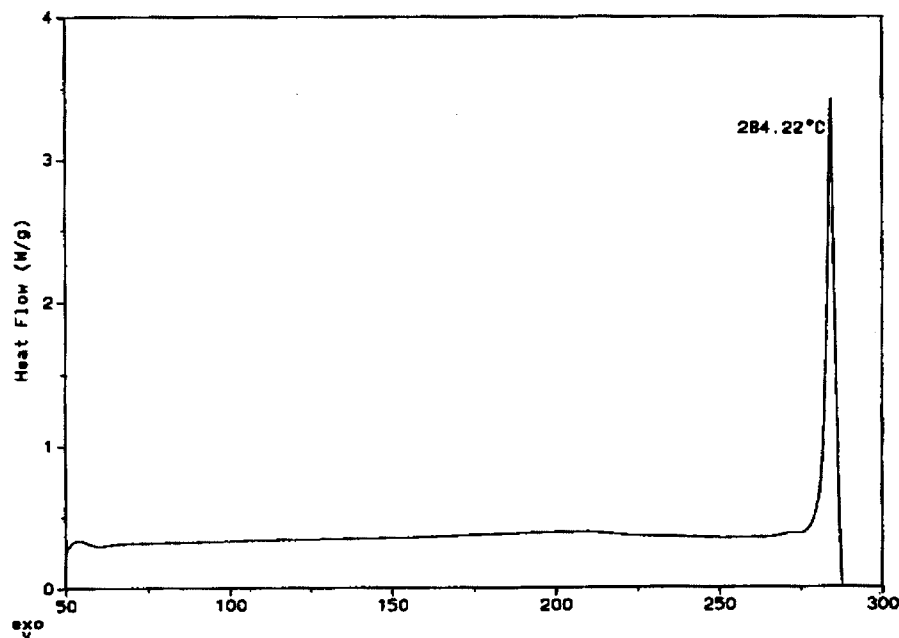


Figure 5 DSC mp of hydrazone IV.

six hydrazones was done with hydrochloric acid as the acid catalyst in an EtOH–THF solvent mixture and a 5% excess of all the carbonyl compounds was used.

The hydrazone incorporation reaction was done in THFA, a high-boiling (178°C) alcohol-ether type solvent. On the basis of the mechanism described in Scheme II, the order of addition of the reactants was chosen carefully to avoid epoxy homopolymerization. First, the hydroxy functionalized hydrazones were stirred in hot THFA, and only after its complete dissolution was the base catalyst, BTMAH, added to generate the phenoxide ion intermediate. EPON 164 was then added slowly in stages; over a period of 45 min, to maintain sufficient phenoxide ion concentration throughout the addition. This ensured opening of the epoxide ring mostly by the hydrazone phenoxide ion, and the occurrence of the self-polymerization of EPON 164, if any, was minimal.

NLO properties of poled NLO I–VI Films

Achieving good long-term thermal stability of poled NLO polymers is critically important for optoelectronic device applications. The most useful measurements of stability are made at or above the highest projected operating temperature for a device application. The dynamic thermal behavior, that is, the monitoring of the NLO properties in real time as the temperature is increased, is a good method to use to study the thermal stability of any NLO-active system. Dynamic measurement is a quick method that indicates the extent to which NLO properties will diminish when the material is taken to high temperatures for a

short period of time, as in device manufacturing. In this measurement, the poled polymer film is heated in a controlled manner while the SHG signal is simultaneously monitored. This technique was applied to the six NLO-active systems prepared for this study. As expected, none of the unpoled samples of NLOs I–VI exhibited any SHG signals.

For ease of comparison, the six NLO-active systems were further divided into two categories. The first category consisted of NLO systems I–III, prepared from hydrazones of 4-NPH. The second category consisted of NLO systems IV–VI, prepared from hydrazones of 2,4-DNPH.

The plots in Figures 6 and 7 depict relative SHG intensity versus temperature for the two categories of compositions. It is apparent from the data that NLOs III and VI, which contained hydrazones derived from 4-hydroxybenzophenone exhibited higher SHG intensities than the corresponding polymers (NLO I and

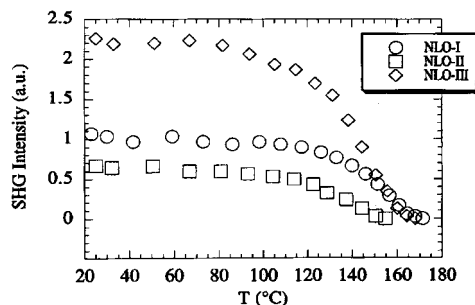


Figure 6 Relative SHG intensity versus temperature profile for NLOs I–III.

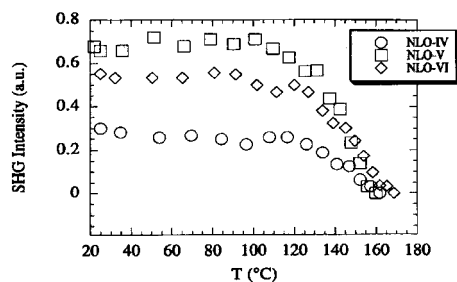


Figure 7 Relative SHG intensity versus temperature profile for NLOs IV–VI.

NLO IV), which were prepared from hydrazones based on 4-hydroxybenzaldehyde. This difference may have been attributable to the greater conjugation provided by the three aromatic rings or to greater planarity of the structure resulting from the steric influences of the rings in NLOs III and VI. (Increasing conjugation length and improving pi orbital overlap were expected to enhance polarizability and, thereby, increase NLO activity.) The results can also be interpreted in another way. The T_g values for NLO I and NLO III were 147.6 and 137.2°C, respectively. A similar difference was observed in the T_g values of NLO IV and NLO VI. The lower T_g values of NLO III and NLO VI may have led to an improved poling efficiency for these materials, resulting in a greater SHG intensity. Similar arguments can be applied to the results observed for prepolymers containing hydrazones derived from 4-hydroxyacetophenone, which displayed the lowest T_g values in each series. However, the general activity of these chromophores were low, possibly because of poorer pi overlap in the methyl-substituted azomethine bond.

A comparison of Figures 6 and 7 also reveals that the SHG values for NLOs I–III, based on 4-NPH, were in some cases significantly higher than the corresponding values for NLOs IV–VI, based on 2,4-DNPH. The latter was a stronger electron acceptor than 4-NPH and should have promoted greater charge separation in the chromophore. This effect was reflected, in fact, in the generally higher mp values of the hydrazones prepared from 2,4-DNPH. However, the greater polarity of the 2,4-DNPH hydrazones may have made them more difficult to orient by poling, explaining the lower SHG activity observed for the NLO IV–VI series.

Figure 8 depicts the normalized dependence of SHG intensity on temperature for NLOs I–III from which the relative depoling temperature, that is, the temperature at which the SHG intensity reached half its maximum intensity, could be determined. The intensities of NLOs I–III were all relatively stable up to 100°C. However, the normalized SHG intensity data for NLO systems IV–VI, shown in Figure 9, indicated that these systems had greater thermal stability than NLO sys-

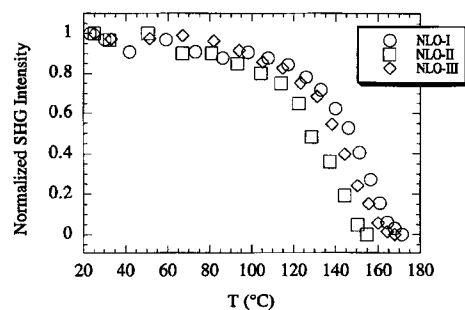


Figure 8 Normalized SHG intensity versus temperature profile for NLOs I–III.

tems I–III, whereas NLOs I–III showed a sharp decay in the SHG signal above 100°C, the SHG signal for NLOs IV–VI was stable up to 120°C. In both instances, the SHG signal decayed rapidly at temperatures approaching 150°C, suggesting that the molecular alignment produced by poling was quickly lost at these temperatures through fast rotation of the chromophores and polymer chain fragments in local areas of high free volume.^{38–41} These results were not surprising in view of the 150°C curing temperature used in the study because the T_g values of high-temperature thermosets tended to approach the highest curing temperature applied to the system. As the T_g approached the curing temperature, reactant mobility was reduced and further crosslinking, which would otherwise increase T_g , was inhibited. A similar effect was observed by White et al.⁴² in their work with novel bifunctional NLO molecules that were poled and simultaneously crosslinked by means of a two-stage reaction with a trifunctional isocyanurate comonomer. White's also suggested that regardless of curing temperature, slow cooling after poling allows densification of the polymer that results in enhanced stability.

Park et al.⁵ also suggested that the effect of epoxy crosslinking–densification process on chromophore mobility was a complex function of crosslinking temperature, stoichiometry, and crosslinking agent. This could be a plausible explanation for the thermal sta-

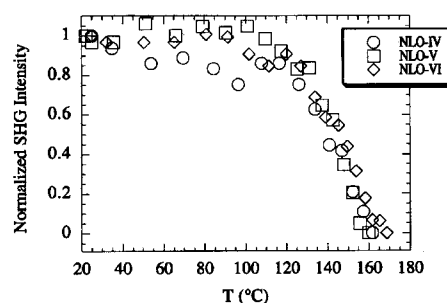


Figure 9 Normalized SHG intensity versus temperature profile for NLOs IV–VI.

bility of NLO systems I–VI because in this study, relatively low poling fields were applied to a single layer to ensure that the film integrity was maintained during poling, and the poling conditions were unoptimized for this study. Park et al. also indicated that it is very reasonable to assume that dangling half-reacted epoxide side chains, that is, incomplete crosslinking, will have a plasticizing effect on the chromophore–polymer matrix.

CONCLUSIONS

Six monohydroxy hydrazones were synthesized in high yield and attached to an epoxy resin matrix to form NLO-active prepolymers. Crosslinked prepolymers containing hydrazones prepared from 4-hydroxybenzophenone exhibited higher SHG intensities than the corresponding structures containing hydrazones prepared from 4-hydroxybenzaldehyde. Likewise, prepolymer systems containing hydrazones prepared from 4-NPH generally showed higher NLO activities than compositions prepared from 2,4-DNPH. Conversely, the overall thermal stability of the latter system was higher by 20°C in comparison to the first group.

The work successfully demonstrated the concept of a thermosetting NLO polymer system comprising a chromophore-attached hydroxyl-functional prepolymer and a blocked polyisocyanate crosslinking agent. By controlling the deblocking temperature of the polyisocyanate, we arranged the poling and curing events to occur in the desired sequence. It should be possible to further enhance the thermal stability of such NLO systems by the addition of a crosslinking site to the chromophore so that after poling and curing, it is effectively attached at two points to the surrounding polymer structure. Two-point attachment of the chromophore versus single-point attachment, as examined here, should inhibit the relaxation processes that reduce second-order NLO activity significantly. In addition, the use of polyisocyanate crosslinking agents, which deblock at temperatures well above the temperature required for efficient poling, should make the poling and curing processes more independent and potentially allow higher T_g values to be achieved.

References

1. Prasad, P. N.; Williams, D. J. In *Introduction to Nonlinear Optical Effects in Molecules*; Wiley: New York, 1991.
2. Singer, K. D.; Sohn, J. E.; Lalama, S. L. *Appl Phys Lett* 1986, 49, 248.
3. Knoesen, A.; Mortazavi, M. A.; Kowel, S. T.; Dienes, A.; Higgins, B. G. *Tech Digest Ser. Opt Soc Am* 1988, 9, 244.
4. Eich, M.; Reck, B.; Yoon, D. Y.; Willson, C. G.; Bjorklund, G. C. *J Appl Phys* 1989, 66, 3241.
5. Park, J.; Marks, T. J.; Yang, J.; Wong, G. K. *Chem Mater* 1990, 2, 229.
6. Chen, M.; Yu, L. P.; Dalton, L. R.; Shi, Y. Q.; Steier, W. H. *Proc SPIE, IntSoc Opt Eng* 1991, 1409, 202.
7. Chen, M.; Yu, L. P.; Dalton, L. R.; Shi, Y. Q.; Steier, W. H. *Macromolecules* 1991, 24, 5421.
8. Shi, Y. Q.; Steier, W. H.; Yu, L. P.; Chen, M.; Dalton, L. R. *Appl Phys Lett* 1991, 58, 1131.
9. Mandal, B. K.; Chen, Y. M.; Lee, J. Y.; Kumar, J.; Tripathy, S. *Appl Phys Lett* 1991, 58, 2459.
10. Jungbauer, D.; Reck, B.; Tweig, R.; Yoon, D. Y.; Willson, C. G.; Swalen, J. D. *Appl Phys Lett* 1990, 56, 2610.
11. Chemla, D. S.; Zyss, J.: In *Nonlinear Optical Properties of Organic Molecules and Crystals*; Academic: Orlando, FL, 1987; Vol. 1, p 227.
12. Bubeck, C.; Laschewsky, A.; Lupo, D.; Neher, D.; Ottenbreit, P.; Paulus, W.; Pass, W.; Ringsdorf, H.; Wegner, G. *Adv Mater* 1991, 3, 54.
13. Hall, S. R.; Kolinsky, P. V.; Jones, R.; Allen, S.; Gordon, P.; Bothwell, B.; Bloor, D.; Norman, P. A.; Hursthouse, M.; Karaulov, A.; Baldwin, J.; Goodyear, M.; Bishop, D. *J Cryst Growth* 1986, 79, 745.
14. Serbutoviez, C.; Bosshard, C.; Knopfle, G.; Wyss, P.; Pretre, P.; Gunter, P.; Schenk, K.; Solan, E.; Chapuis, G. *Chem Mater* 1995, 7, 1198.
15. Kurtz, S. K.; Perry, T. T. *J Appl Phys* 1968, 39, 3798.
16. Zyss, J.; Ledoux, I.; Nicoud, J. F. In *Molecular Nonlinear Optics*; Zyss, J., Ed.; Academic: New York, 1993; p 148.
17. Bolognesi, G. P.; Mezzetti, S.; Pandarese, F. *Opt Commun*, 1973, 8, 267.
18. Pandarese, F.; Panizza, S.; Telo, A. *Opt Commun* 1974, 12, 14.
19. Bertinelli, F.; Taliani, C. *Chem Phys Lett* 1974, 28, 231.
20. Owen, J. R.; White, E. A. D. *J Mater Sci Lett* 1976, 11, 2165.
21. Kminek, I.; Nespurek, S. *Polym Bull* 1974, 32, 573.
22. Goddu, R. F.; Delker, D. A. *Anal Chem* 1958, 30, 2013.
23. Dannenberg, H. *Soc Plast Eng Trans* 1963, 3, 78.
24. Schiering, D. W.; Katon, J. E. *J Appl Polym Sci* 1987, 34, 2367.
25. Mijovic, J.; Andjelic, S. *Macromolecules* 1995, 28, 2787.
26. Mijovic, J.; Andjelic, S.; Winnie Yee, C. F. *Macromolecules* 1995, 28, 2797.
27. Mortazavi, M.; Knoesen, A.; Kowel, S.; Higgings, B.; Dienes, A. *J Opt Soc Am B* 1989, 6, 733.
28. Hampsch, H. L.; Torkelson, J.; Bethke, S.; Grubb, S. *J Appl Phys* 1990, 67, 1037.
29. Knoesen, A.; Molau, N.; Yankelevich, D.; Mortazavi, M.; Dienes, A. *Int J Nonlinear Opt Phys* 1992, 1, 73.
30. Karabatsos, G. J.; Vane, F. M.; Taller, R. A.; His, N. *J Am Chem Soc* 1964, 86, 3351.
31. Karabatsos, G. J.; Graham, J. D.; Vane, F. M. *J Am Chem Soc* 1962, 84, 753.
32. Allen, C. F. H.; Richmond, J. H. *J Org Chem* 1937, 2, 222.
33. Bryant, W. M. A. *J Am Chem Soc* 1936, 58, 2335.
34. Campbell, N. *Analyst* 1936, 61, 391.
35. Bredereck, S. *Ber* 1932, 65, 1833.
36. Johnson, G. D. *J Am Chem Soc* 1953, 75, 2720.
37. Shine, H. J. *J Org Chem* 1959, 24, 252.
38. Struik, L. C. E. *Polymer* 1987, 28, 57.
39. Robertson, R. E.; Shimha, R.; Curro, J. C. *Macromolecules* 1984, 17, 119.
40. Chow, T. S. *Macromolecules* 1984, 17, 2336.
41. Oliver, N. H.; Pecora, R.; Ouano, A. C. *Macromolecules* 1985, 18, 2208.
42. White, K. M.; Francis, C. V.; Isackson, A. J. *Macromolecules* 1994, 27, 3619.